n-Type Conjugated Oligoquinoline and Oligoquinoxaline with Triphenylamine Endgroups: Efficient Ambipolar Light Emitters for Device Applications

Jessica M. Hancock, Angela P. Gifford, Yan Zhu, Yun Lou, and Samson A. Jenekhe*

Department of Chemical Engineering and Department of Chemistry, University of Washington, Seattle, Washington 98195-1750

Received June 13, 2006. Revised Manuscript Received August 4, 2006

New n-type conjugated oligomers with p-type endgroups, 2,2′-bis(triphenylamine)-4,4′-diphenyl-[6,6′]-biquinoline (TPA-2PQ, **3**) and 2,2′-bis(triphenylamine)-3,3′-diphenyl-[6,6′]biquinoxaline (TPA-2PQx, **6**), were synthesized, characterized, and found to be efficient ambipolar blue-green and pure green emitters in organic light-emitting diodes (OLEDs). In toluene solution, oligoquinoline TPA-2PQ emitted blue-green fluorescence with a quantum yield of 62% and a lifetime of 1.3 ns, whereas the oligoquinoxaline TPA-2PQx emitted green fluorescence with a 34% quantum yield and a lifetime of 5.3 ns. Both oligomers showed ambipolar redox properties, identical HOMO levels at 5.31 eV, and LUMO levels of 2.59 eV for TPA-2PQ and 2.92 eV for TPA-2PQx. Bright green electroluminescence (up to 15 330 cd/m^2) with high efficiency (up to 7.9 cd/A and 3.0% external quantum efficiency) were achieved from TPA-2PQx as the emitter in OLEDs. Despite its better fluorescence quantum yield, blue-green electroluminescence with far lower brightnesses (up to 6850 cd/m^2) and efficiencies (up to 2.7 cd/A) were obtained from the oligoquinoline (TPA-2PQ) emitter. The substantially better device performance of the oligoquinoxaline as well as the variation in OLED color among the two oligomers can be understood from their 0.33 eV difference in electron affinity, which favors improved electron injection/transport and confinement in the oligoquinoxaline. These results show that n-type oligomers with p-type endgroups represent a promising approach to efficient ambipolar emitters for OLEDs.

Introduction

Molecular semiconductors being developed for diverse applications in organic electronics,[1] including light-emitting diodes, thin film transistors, and photovoltaic cells, fall broadly into three structural classes: small molecules,[2] conjugated polymers,[3] and conjugated oligomers.[4] Monodisperse oligomers are especially attractive in that they can combine the well-defined size and structure of small molecules with the improved thermal resistance and good mechanical properties of polymers. Both as model systems for the related conjugated polymers and as active semiconductors in electronic devices, a large number of different classes of p-type (electron donor) conjugated oligomers have been studied, most notably oligothiophenes,[4,5] oligophenylenes,[4,6] oligophenylenevinylene,[4,7] oligoacenes,[4,8] and oligofluorenes.[9] Although several classes of n-type conjugated polymers are known, for example, the polyquinolines,[10] polyquinoxalines,[11] and polyanthrazolines,[10] few examples of n-type conjugated oligomers[12] are known.

The need to develop more efficient light emitters for organic light-emitting diodes (OLEDs) has resulted in the exploration of various approaches to the design of multi-

* To whom correspondence should be addressed. E-mail: jenekhe@u.washington.edu. Fax: 206-685-3451.

(1) See the special issue on Organic Electronics: *Chem. Mater.* **2004**, *16*, 4381−4846.

(2) (a) Tang, C. W.; VanSlyke, S. A. *Appl. Phys. Lett.* **1987**, *51*, 913. (b) Mitschke, U.; Bauerle, P. *J. Mater. Chem.* **2000**, *10*, 1471. (c) Chen, C. T. *Chem. Mater.* **2004**, *16*, 4389. (d) Shirota, Y. *J. Mater. Chem.* **2000**, *10*, 1. (d) Shah, B. K.; Neckers, D. C.; Shi, J. M.; Forsythe, E. W.; Morton, D. *Chem. Mater.* **2006**, *18*, 603.

(3) (a) Friend, R. H.; Gymer, R. W.; Holmes, A. B.; Burroughs, J. H.; Marks, R. N.; Taliani, C.; Bradley, D. D. C.; Dos Santos, D. A.; Brédas, J. L.; Lögdlund, M.; Salaneck, W. R. *Nature* **1999**, *397*, 121. (b) Kraft, A.; Grimsdale, A. C.; Holmes, A. B. *Angew. Chem., Int. Ed.* **1998**, *37*, 402. (c) Heeger, A. J. *Solid State Commun.* **1998**, *107*, 673. (d) Kulkarni, A. P.; Tonzola, C. J.; Babel, A.; Jenekhe, S. A. *Chem. Mater.* **2004**, *16*, 4556. (e) Yan, H.; Lee, P.; Armstrong, N. R.; Graham, A.; Evmenenko, G. A.; Dutta, P.; Marks, T. J. *J. Am. Chem. Soc.* **2005**, *127*, 3172. (f) Furuta, P. T.; Deng, L.; Garon, S.; Thompson, M. E.; Frechet, J. M. J. *J. Am. Chem. Soc.* **2004**, *126*, 15388. (g) Kulkarni, A. P.; Zhu, Y.; Jenekhe, S. A. *Macromolecules* **2005**, *38*, 1553.

(4) (a) *Electronic Materials: The Oligomer Approach*; Mullen, K.; Wegner, G., Eds.; Wiley-VCH: Weinheim, Germany, 1998. (b) Martin, R. E.; Diederich, F. *Angew. Chem., Int. Ed.* **1999**, *38*, 1350.

(5) (a) Garnier, F.; Yassar, A.; Hajlaoui, R.; Horowitz, G.; Deloffre, F.; Servet, B.; Ries, S.; Alnot, P. *J. Am. Chem. Soc.* **1993**, *115*, 8716. (b) Facchetti, A.; Yoon, M. H.; Stern, C. L.; Hutchison, G. R.; Ratner, M. A.; Marks, T. J. *J. Am. Chem. Soc.* **2004**, *126*, 13480.

(6) (a) Tour, J. M. *Adv. Mater.* **1994**, *6*, 190. (b) Muller, M.; Kubel. C.; Mullen, K. *Chem.—Eur. J.* **1998**, *4*, 2099.

(7) (a) Wang, S. J.; Bazan, G. C.; Tretiak, S.; Mukamel, S. *J. Am. Chem. Soc.* **2000**, *122*, 1289. (b) Robinson, M. R.; Wang, S.; Bazan, G. C.; Cao, Y. *Adv. Mater.* **2000**, *12*, 1701. (c) Wong, M. S.; Li, Z. H.; Tao, Y.; D'Iorio, M. *Chem. Mater.* **2003**, *15*, 1198.

(8) (a) Jang, B. B.; Lee, S. H.; Kafafi, Z. H. *Chem Mater.* **2006**, *18*, 449. (b) Cheng, Y. C.; Silbey, R. J.; da Silva, D. A.; Calbert, J. P.; Cornil, J.; Bredas, J. L. *J. Chem. Phys.* **2003**, *118*, 3764. (c) Hummer, K.; Ambrosch-Draxl, C. *Phys. Rev. B* **2005**, *71*, 081202. (d) Kelley, T. W.; Baude, P. F.; Gerlach, C.; Ender, D. E.; Muyres, D.; Haase, M. A.; Vogel, D. E.; Theiss, S. D. *Chem. Mater.* **2004**, *16*, 4413.

(9) (a) Geng, Y.; Trajkovska, A.; Katsis, D.; Ou, J. J.; Culligan, S. W.; Chen, S. H. *J. Am. Chem. Soc.* **2002**, *124*, 8337. (b) Geng, Y.; Chen, A. C. A.; Ou, J. J.; Chen, S. H.; Klubek, K.; Vaeth, K. M.; Tang, C. W. *Chem. Mater.* **2003**, *15*, 4352. (c) Chi, C. Y.; Wegner, G. *Macromol. Rapid Commun.* **2005**, *26*, 1532. (d) Kulkarni, A. P.; Kong, X.; Jenekhe, S. A. *J. Phys. Chem. B* **2004**, *108*, 8689. (e) Belfield, K. D.; Morales, A. R.; Hales, J. M.; Hagan, D. J.; Van Stryland, E. W.; Chapela, V. M.; Percino, J. *Chem. Mater.* **2004**, *16*, 2267.

10.1021/cm0613760 CCC: $33.50
Published on Web 09/12/2006

functional materials with donor−acceptor (D−A) architecture capable of ambipolar charge transport and high luminescence efficiency.[2d,13−15] Numerous emissive D−A small molecules for OLEDs have been reported.[2d,13−15] Many conjugated polymers with donor−acceptor architecture of the type poly(D−A) have also been investigated.[16] Although they can exhibit ambipolar charge transport and redox properties, the luminescence quantum yields of such polymers tend to be small because of the rather large intramolecular charge transfer (ICT).[16] p-Type conjugated polymers, poly(D), with acceptor (A) side chains represent another strategy toward ambipolar light emitters;[3d,17] however, the complexity of these latter materials and the difficulties in their syntheses are drawbacks. Here, we propose that conjugated oligomers with donor−acceptor architecture, e.g., D−$(A)_x$−D or A−$(D)_x$−A, offer an attractive alternative approach to the design of efficient ambipolar light emitters for OLEDs.

In this paper, we report the synthesis and investigation of new oligomers with donor−acceptor structure as ambipolar light emitters for OLEDs. The molecular structures of the n-type oligomers with p-type (donor) endgroups, 2,2′-bis(triphenylamine)-4,4′-diphenyl-[6,6′]biquinoline (TPA-2PQ, **3**) and 2,2′-bis(triphenylamine)-3,3′-diphenyl-[6,6′]biquinoxaline (TPA-2PQx, **6**), are shown in Chart 1. The endgroups in both oligomers are triphenylamines (TPA), a well-known donor moiety that can endow or enhance transport of holes.[18] Oligoquinolines and polyquinolines have previously been demonstrated as electron transport (n-type) materials for OLEDs.[10] Polyquinoxalines have also previously been reported as good electron-transport materials for OLEDs.[11] The ambipolar redox properties of the new oligomers were investigated by cyclic voltammetry and related HOMO/LUMO levels were estimated. The photophysical properties in solution and in thin films were investigated by steady-state photoluminescence (PL) spectroscopy and by measuring the PL decay dynamics. Electroluminescence (EL) devices using the new oligomers as emitters were fabricated and evaluated.

Chart 1

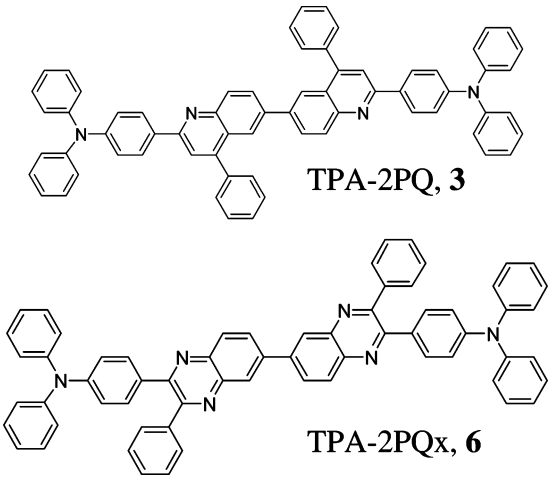

Results and Discussion

Synthesis and Characterization. Oligoquinoline TPA-2PQ (**3**) was obtained in 68% yield by acid-catalyzed Friedlander condensation of 1-(4-diphenylamino-phenyl)-ethanone (**1**) with 3,3′-dibenzoylbenzidine (**2**), as outlined in Scheme 1. The diphenyl phosphate (DPP) catalyst was readily removed by precipitation into 10% triethylamine/ethanol solution. The synthetic route to oligoquinoxaline **6** (TPA-2PQx) is shown in Scheme 2. The α,β-diketone **5** was obtained in two steps, Sonogashira coupling of phenylacetylene with 4-bromo-*N*,*N*-diphenylaniline followed by oxidation of the triple bond in **4**. Condensation of the α,β-diketone **5** with 3,3′-diaminobenzidine gave the oligoquinoxaline in 45% yield. Both oligomers **3** and **6** were purified by column chromatography. ^{1}H NMR spectroscopy, high-resolution mass spectrometry (HRMS), and FTIR were used to confirm the structures of the oligomers. The electrochemical and photophysical properties discussed later also confirmed the molecular structures of these compounds.

Thermogravimetric analysis (TGA) showed that the onset decomposition temperature (T_D) of the oligomers was quite high, 450 °C for TPA-2PQ and 531 °C for TPA-2PQx. The differential scanning calorimetry (DSC) of these oligomers showed robust thermal resistance characteristics. Oligoquinoline TPA-2PQ had a glass-transition temperature (T_g) of 245

(10) (a) Zhang, X.; Shetty, A. S.; Jenekhe, S. A. *Macromolecules* **1999**, *32*, 7422. (b) Zhang, X.; Jenekhe, S. A. *Macromolecules* **2000**, *33*, 2069. (c) Zhu, Y.; Alam, M. M.; Jenekhe, S. A. *Macromolecules* **2003**, *36*, 8958. (d) Jenekhe, S. A.; Zhang, X.; Chen, X. L.; Choong, V.-E.; Gao, Y.; Hsieh, B. R. *Chem. Mater.* **1997**, *9*, 409. (e) Tonzola, C. J.; Alam, M. M.; Jenekhe, S. A. *Adv. Mater.* **2002**, *14*, 1086. (f) Tonzola, C. J.; Alam, M. M.; Jenekhe, S. A. *Macromolecules* **2005**, *38*, 9539.

(11) (a) Yamamoto, T.; Sugiyama, K.; Kushida, T.; Inoue, T.; Kanbara, T. *J. Am. Chem. Soc.* **1996**, *118*, 3930. (b) O'Brien, D.; Weaver, M. S.; Lidzey, D. G.; Bradley, D. D. C. *Appl. Phys. Lett.* **1996**, *69*, 881. (c) Jandke, M.; Strohriegl, P.; Berleb, S.; Werner, E.; Brütting, W. *Macromolecules* **1998**, *31*, 6434. (d) Cui, Y.; Zhang, X.; Jenekhe, S. A. *Macromolecules* **1999**, *32*, 3824. (e) Jung, S.-H.; Kim, D. Y.; Cho, H.-N.; Suh, D. H. *J. Polym. Sci., Part A: Polym. Chem.* **2006**, *44*, 1189.

(12) (a) Kulkarni, A. P.; Gifford, A. P.; Tonzola, C. J.; Jenekhe, S. A. *Appl. Phys. Lett.* **2005**, *86*, 061106. (b) Tonzola, C. J.; Hancock, J. M.; Babel, A.; Jenekhe, S. A. *Chem. Commun.* **2005**, 5214. (c) Shetty, A. S.; Liu, E. B.; Lachicotte, R. J.; Jenekhe, S. A. *Chem. Mater.* **1999**, *11*, 2292.

(13) (a) Shirota, Y.; Kinoshita, M.; Noda, T.; Okumoto, K.; Ohara, T. *J. Am. Chem. Soc.* **2000**, *122*, 11021. (b) Doi, H.; Kinoshita, M.; Okumoto, K.; Shirota, Y. *Chem. Mater.* **2003**, *15*, 1080. (c) Tamoto, N.; Adachi, C.; Nagai, K. *Chem. Mater.* **1997**, *9*, 1077.

(14) (a) Kulkarni, A. P.; Wu, P.-T.; Kwon, T. W.; Jenekhe, S. A. *J. Phys. Chem. B* **2005**, *109*, 19584. (b) Zhu, Y.; Kulkarni, A. P.; Jenekhe, S. A. *Chem. Mater.* **2005**, *17*, 5225. (c) Kulkarni, A. P.; Kong, X.; Jenekhe, S. A. *Adv. Funct. Mater.* **2006**, *16*, 1057. (d) Lai, R. Y.; Fabrizio, E. F.; Lu., L.; Jenekhe, S. A.; Bard, A. J. *J. Am. Chem. Soc.* **2001**, *123*, 9112.

(15) (a) Thomas, K. R. J.; Lin, J. T.; Tao, Y.-T.; Chuen, C.-H. *Chem. Mater.* **2002**, *14*, 3852. (b) Thomas, K. R. J.; Velusamy, M.; Lin, J. T.; Chuen, C.-H.; Tao, Y.-T. *Chem. Mater.* **2005**, *17*, 1860. (c) Thomas, K. R. J.; Lin, J. T.; Velusamy, M.; Tao, Y.-T.; Chuen, C.-H. *Adv. Funct. Mater.* **2004**, *14*, 83. (d) Chen, S.; Xu, X.; Liu, Y.; Yu, G.; Sun, X.; Qiu, W.; Ma, Y.; Zhu, D. *Adv. Funct. Mater.* **2005**, *15*, 1541.

(16) (a) Jenekhe, S. A.; Lu, L.; Alam, M. M. *Macromolecules* **2001**, *34*, 7315. (b) Champion, R. D.; Cheng, K.-F.; Pai, C.-L.; Chen, W.-C.; Jenekhe, S. A. *Macromol. Rapid Commun.* **2005**, *26*, 1835. (c) Yamamoto, T.; Yasuda, T. Sakai, Y.; Aramaki, S. *Macromol. Rapid Commun.* **2005**, *26*, 1214.

(17) (a) Bao, Z.; Peng, Z. H.; Galvin, M. E.; Chandross, E. A. *Chem. Mater.* **1998**, *10*, 1201. (b) Lee, Y.-Z.; Chen, X.; Chen, S. A.; Wei, P.-K.; Fann, W.-S. *J. Am. Chem. Soc.* **2001**, *123*, 2296. (c) Kim, J. H.; Park, J. H.; Lee. H. *Chem. Mater.* **2003**, *15*, 3414.

(18) (a) Bender, T. P.; Graham, J. F.; Duff, J. M. *Chem. Mater.* **2001**, *13*, 4105. (b) Casalbore-Miceli, G.; Esposti, A. D.; Fattori, V.; Marconi, G.; Sabatini, C. *Phys. Chem. Chem. Phys.* **2004**, *6*, 3092.

Scheme 1. Synthesis of Oligoquinoline TPA-2PQ (3)

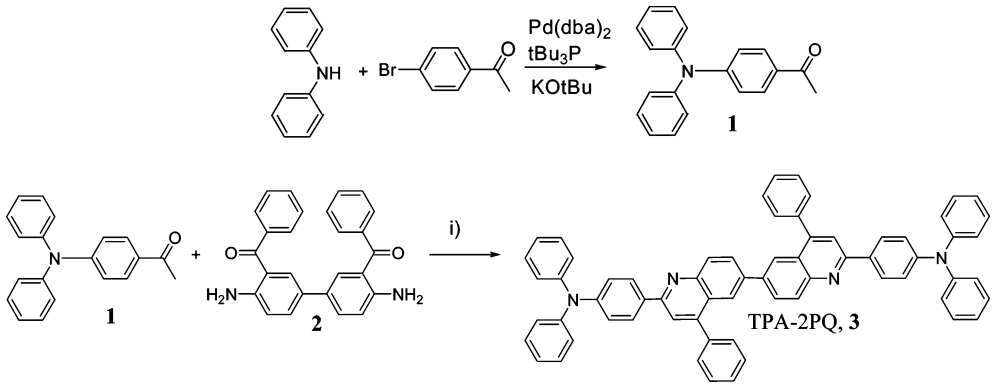

i) diphenyl phosphate (DPP), 140 ° C, 24 h.

Scheme 2. Synthesis of Oligoquinoxaline TPA-2PQx (6)

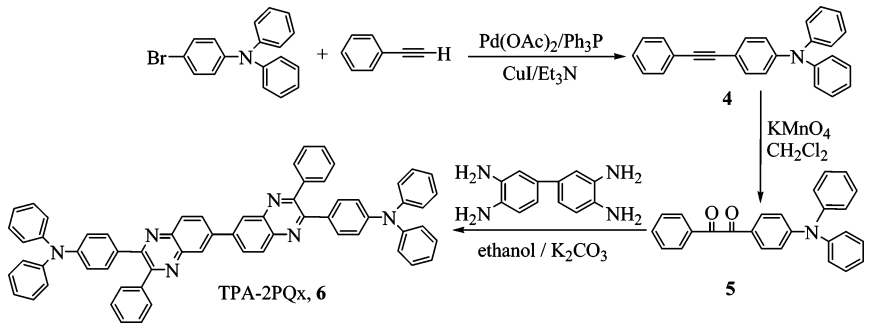

°C and a melting temperature (T_m) of 330 °C. Oligoquinoxaline TPA-2PQx had a T_g of 148 °C, a broad crystallization peak at 218 °C, and a T_m of 311 °C. The high glass-transition temperatures and overall robust thermal-resistance properties of these oligomers are in accord with the known features of polyquinolines[10] and polyquinoxalines.[11]

Electrochemical Properties. The cyclic voltammograms (CVs) of TPA-2PQ and TPA-2PQx in benzene/acetonitrile (1.5:1 v/v) are shown in Figure 1. The oxidation waves in the CVs of TPA-2PQ and TPA-2PQx are nearly identical, as expected because the oligomers have the same triphenylamine (TPA) endgroups. The oxidation CV of TPA-2PQ is characterized by two overlapping reversible waves with half-wave potentials of +0.90 and +1.03 V vs SCE. In TPA-2PQx, the overlapping reversible oxidation waves have half-wave potentials of +0.93 and +1.11 V vs SCE. These values are in good agreement with the reported values of the oxidation potential of TPA (+0.95 V vs SCE; +1.13 V vs Ag/Ag^+).[18] From the half-wave potentials of the first oxidation waves, we estimated the ionization potentials (IP $= E_{1/2} + 4.4$)[3d] of TPA-2PQ and TPA-2PQx to be identical at 5.31 eV.

The reduction CV of TPA-2PQ revealed two reversible reduction waves with half-wave potentials of −1.81 and −1.95 V vs SCE. These values are very close to the reported reduction potential of the monomeric phenylquinoline (PQ) ($E_{1/2} = -1.99$ V).[19] The more positive reduction potential of oligoquinoline TPA-2PQ compared to PQ suggests that the two PQ groups in TPA-2PQ are not electronically decoupled, and that the two waves represent individual reduction of each PQ in the oligomer at a slightly different potential. Similar size-dependent redox properties have been observed in oligofluorenes.[9c] An electron affinity (EA) of 2.59 eV (EA $= E_{1/2} + 4.4$)[3d] was estimated from the half-wave potential of the first reduction wave of TPA-2PQ. Similarly, two reversible reduction waves were observed in the CV of TPA-2PQx with half-wave potentials of −1.48 and −1.67 V vs SCE. The significantly more positive reduction potential of TPA-2PQx compared to TPA-2PQ is due to the stronger electron-accepting character of phenylquinoxaline (PQx) than phenylquinoline. The estimated EA value of TPA-2PQx is 2.92 eV, which is 0.33 eV larger than that of TPA-2PQ. The observed redox properties of these n-type oligomers with p-type endgroups clearly establish their potential to capture (or trap) both electrons and holes. This suggests that the new oligomers could be useful ambipolar materials for OLEDs.

Photophysical Properties. The dilute solution absorption spectra of TPA-2PQ and TPA-2PQx in toluene are shown in Figure 2. TPA-2PQ has its lowest-energy absorption band centered at 441 nm ($\log \epsilon = 4.99$), where ϵ is the molar absorption coefficient, and an additional band with lower intensity at 299 nm ($\log \epsilon = 4.87$). TPA-2PQx has a large intensity band at 299 nm ($\log \epsilon = 5.11$), and two absorption bands of similar intensity centered at 349 nm ($\log \epsilon = 4.94$) and 419 nm ($\log \epsilon = 4.90$). The highest-energy absorption bands in these oligomers can be associated with $\pi-\pi^*$ transitions. The lowest-energy absorption bands in TPA-2PQ and TPA-2PQx can be assigned to the intramolecular charge transfer (ICT) transition $^1CT \leftarrow S_o$. A notable difference in

(19) Agrawal, A. K.; Jenekhe, S. A. *Chem. Mater.* **1996**, *8*, 579.

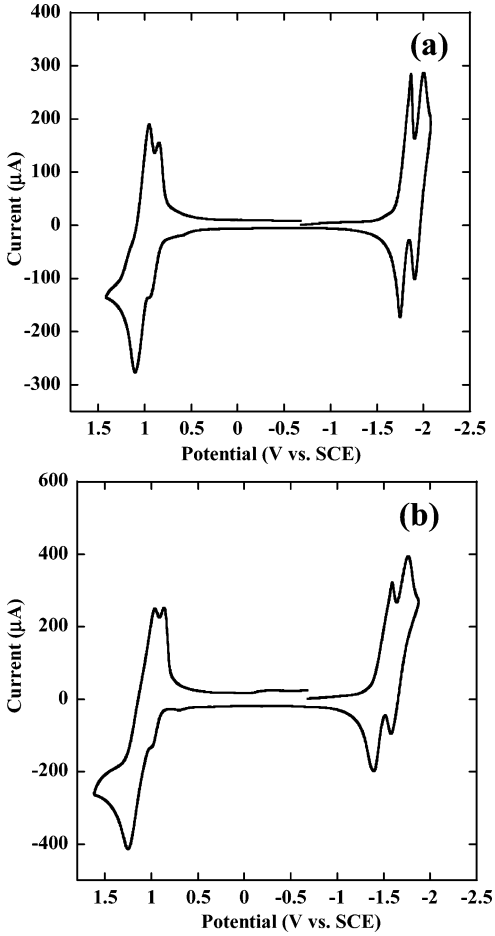

Figure 1. Cyclic voltammograms of 2mM (a) TPA-2PQ and (b) TPA-2PQx in 1.5:1 (v/v) benzene:acetonitrile, 0.1 M $TBPAPF_6$, scan rate = 200 mV/s.

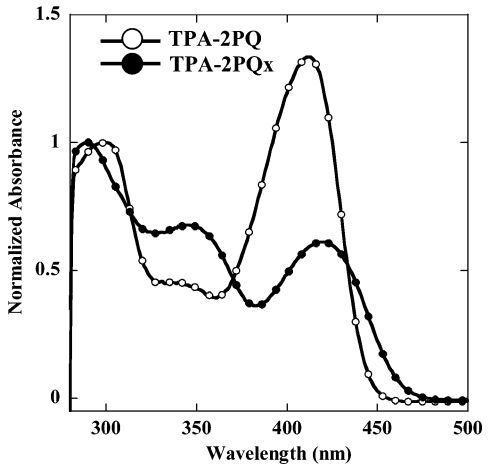

Figure 2. Absorption spectra of TPA-2PQ and TPA-2PQx in dilute toluene solution (5×10^{-5} M).

the absorption spectra of the two oligomers is that the oscillator strength of the ICT absorption band of TPA-2PQ ($\log \epsilon = 4.99$) is larger than that of TPA-2PQx ($\log \epsilon = 4.90$). The larger oscillator strength suggests that there is a higher probability for the $^1CT \leftarrow S_o$ transition in TPA-2PQ. In addition, the ICT band of TPA-2PQx is red-shifted 8 nm from that of TPA-2PQ, indicating a stronger ICT, as expected from the stronger electron-accepting quinoxaline rings relative to the quinoline rings.

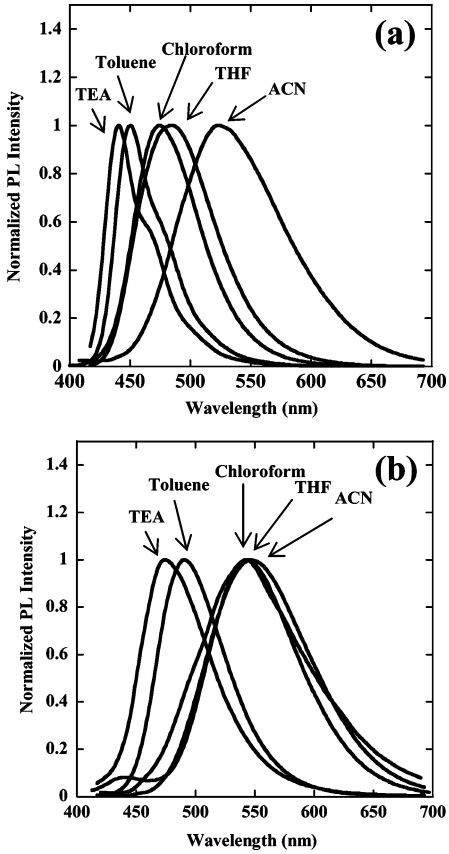

Figure 3. PL emission spectra (400 nm excitation) of oligomers in solvents of various polarity: (a) TPA-2PQ and (b) TPA-2PQx.

The solution photoluminescence (PL) emission spectra of TPA-2PQ and TPA-2PQx in solvents of varying polarity are shown in Figure 3, parts a and b, respectively. The PL emission maximum (λ_{max}^{em}), full width at half-maximum (fwhm), and other photophysical properties in several solvents of varying polarity are collected in Table 1. These results reveal a large positive solvatochromism in the PL emission spectra of both oligomers. However, solvatochromic trends were not observed in the ICT absorption band of TPA-2PQ and TPA-2PQx (Table 1), indicating the absence of significant dipole moments in the ground state. In nonpolar triethylamine (TEA), TPA-2PQ had a λ_{max}^{em} of 441 nm and a fwhm = 43 nm. These values increased to a λ_{max}^{em} of 524 nm and a fwhm of 103 nm in high-polarity acetonitrile (ACN). The λ_{max}^{em} of TPA-2PQx varied from 474 nm (fwhm = 66 nm) in nonpolar TEA to 543 nm (fwhm = 109 nm) in polar ACN. In each solvent, the PL emission spectrum of TPA-2PQx was red-shifted by 20−90 nm and broader by 6−27 nm relative to that of TPA-2PQ. The red-shifted absorption and PL emission of TPA-2PQx relative to TPA-2PQ is consistent with a larger dipole moment of the ^1CT excited state, i.e., stronger ICT effects, in TPA-2PQx because of the larger electron affinity of oligoquinoxaline relative to oligoquinoline and the identical electron-donor endgroups in both oligomers.

A large positive solvatochromism was observed in the Stokes shifts of the solution PL emission spectra of both TPA-2PQ and TPA-2PQx (Table 1). In the case of TPA-2PQ, the Stokes shift increased from 34 nm in TEA to 123 nm in ACN. A larger Stokes shift was exhibited by TPA-

Table 1. Photophysical Properties of TPA-2PQ and TPA-2PQx in Solvents of Various Polarity

oligomer	solvent[a]	ϵ'[b]	λ_{max}^{abs} (nm)	λ_{max}^{em} (nm)	fwhm (nm)	Stokes shift (nm)
TPA-2PQ (**3**)	TEA	2.4	300, 407	441	43	34
	toluene	2.4	297, 412	451	47	39
	chloroform	5.5	300, 406	475	61	69
	THF	7.5	296, 408	484	75	76
	ACN	36.6	303, 401	524	103	123
TPA-2PQx (**6**)	TEA	2.4	346, 415	474	66	59
	toluene	2.4	347, 417	491	66	74
	chloroform	5.5	350, 425	543	88	118
	THF	7.5	342, 414	546	101	132
	ACN	36.6	336, 410	543	109	133

[a] Triethylamine (TEA); tetrahydrofuran (THF); acetonitrile (ACN). [b] ϵ' = dielectric constant of solvent.

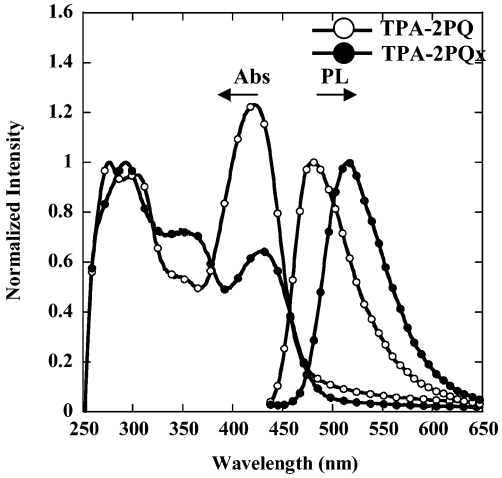

Figure 4. Absorption and PL emission spectra of thermally evaporated thin films of TPA-2PQ and TPA-2PQx.

2PQx, varying from 59 nm in TEA to 133 nm in ACN, providing further evidence of a larger excited-state dipole moment in the oligoquinoxaline compared to the oligoquinoline.

The fluorescence quantum yield (ϕ_f) of the oligomers was measured in toluene solution and found to be 62% for TPA-2PQ and 34% for TPA-2PQx. The much lower ϕ_f value in TPA-2PQx is in agreement with the observed larger ICT strength and lower oscillator strength of the $^1CT \leftarrow S_o$ transition. For more information on the dynamics of the $^1CT \rightarrow S_o$ emission, the PL decay lifetimes of the oligomers were measured in dilute toluene solution (5×10^{-6} M). The PL decays of both TPA-2PQ and TPA-2PQx were well-described by single-exponential fits; the goodness of the fit was characterized by χ^2 values of 1.1−1.6 and Durbin−Watson values of 1.4−2.0. TPA-2PQ had a PL lifetime (τ) of 1.3 ns, whereas it was 5.3 ns in TPA-2PQx. These excited-state lifetimes, on the 1−5 ns scale, are consistent with expectations for charge-transfer excitons.[16a]

Figure 4 shows the normalized optical absorption and PL emission spectra of thermally evaporated TPA-2PQ and TPA-2PQx thin films. Thin films of TPA-2PQ had absorption peaks at 276, 306, and 421 nm, and TPA-2PQx thin films had absorption peaks at 295, 352, and 429 nm. As previously established for the spectra in solution, the lowest-energy absorption band in the thin films is of charge-transfer character. The optical absorption edge band gaps are 2.59 and 2.51 eV for TPA-2PQ and TPA-2PQx, respectively. The thin film PL emission maxima of TPA-2PQ and TPA-2PQx are 480 and 515 nm, respectively. Thin films of TPA-2PQ emit blue-green light with Commission International d'Eclairage (CIE) coordinates of (0.18, 0.36). Because of the stronger ICT character of TPA-2PQx, the thin-film emission is red-shifted to the green region with CIE coordinates of (0.27, 0.59). The PL emission bands of TPA-2PQ and TPA-2PQx thin films originate from ICT excited states, as previously shown from the strong positive solvatochromism in solution (Table 1, Figure 2). The PL decay of the oligomers in the solid state was best described by a biexponential fit. TPA-2PQ had a dominant τ of 0.53 ns with a relative amplitude of 98% and exhibited a long-lived excited state-species with a τ of 2.0 ns ($\chi^2 = 1.0$, Durbin−Watson = 1.9). TPA-2PQx had a short lifetime component of 0.75 ns with a relative amplitude of 58% and a long lifetime component of 3.7 ns with a relative amplitude of 42% ($\chi^2 = 1.0$, Durbin−Watson = 2.0). The large difference between the dominant PL lifetimes of the oligomers in solution and solid state suggests complications due to intermolecular interactions or morphology. In the case of oligoquinoxaline TPA-2PQx, two significant excited-state species are implied by the observed two PL lifetimes. One of these excited-state species is clearly the same as the CT state observed in solution. The other component is possibly due to intermolecular excimers commonly observed in related conjugated polymers[20] or a consequence of different CT species in different solid-state conformations.

Light-Emitting Diodes. OLEDs of different architectures, based on the oligomers TPA-2PQ and TPA-2PQx, were fabricated and evaluated in ambient air. Five different device structures were investigated:[21] ITO/oligomer/LiF/Al (diode I), ITO/PEDOT/PVK/oligomer/LiF/Al (diode II), ITO/PEDOT/PVK/oligomer/TPBI/LiF/Al (diode III), ITO/PEDOT/TAPC/oligomer/LiF/Al (diode IV), and ITO/PEDOT/TAPC/oligomer/TPBI/LiF/Al (diode V). Single-layer OLEDs (diode I) had uniform electroluminescence (EL), and the EL spectra of TPA-2PQ and TPA-2PQx, shown in Figure 5, are identical to the corresponding thin-film PL emission spectra. The EL emission of TPA-2PQ was blue-green in color and had a maximum at 470 nm and CIE coordinates of (0.18, 0.22). The single-layer OLEDs based on TPA-2PQx emitted pure green with an EL maximum at 505 nm and CIE coordinates of (0.19, 0.55). The spectrally identical EL and PL emission spectra of both TPA-2PQ and

(20) Jenekhe, S. A.; Osaheni, J. A. *Science* **1994**, *265*, 765.
(21) Indium tin oxide (ITO); poly(ethylenedioxythiophene)/poly(styrene sulfonate) blend (PEDOT); poly(*N*-vinylcarbozole) (PVK); 1,1-bis-(di-4-tolylaminophenyl)cyclohexane (TAPC); 1,3,5-tris(N-phenylbenzimidizol-2-yl)benzene (TPBI).

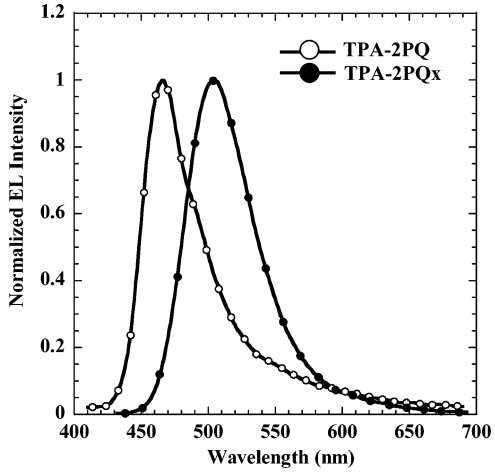

Figure 5. EL spectra of TPA-2PQ and TPA-2PQx diodes (ITO/oligomer/LiF/Al).

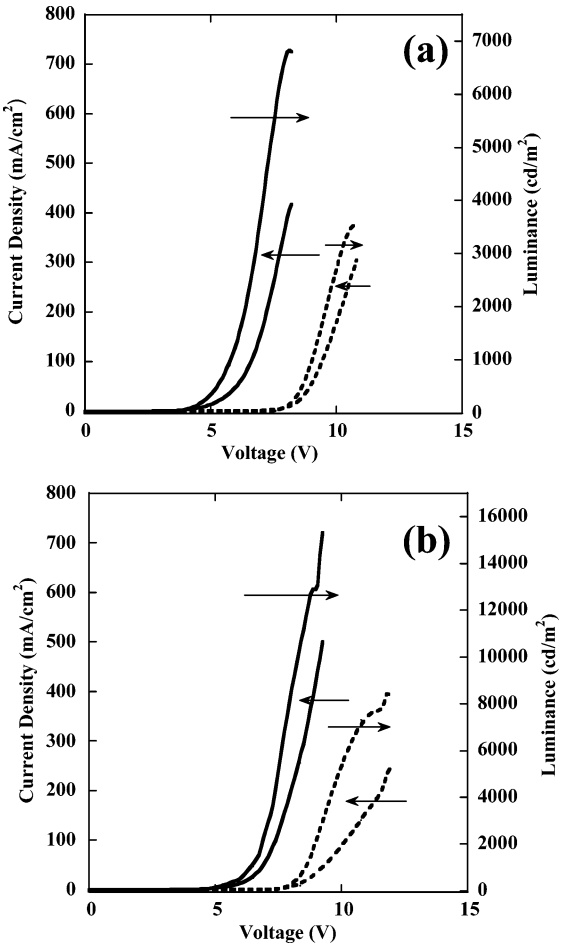

Figure 6. Luminance−current density−voltage characteristics of (a) TPA-2PQ and (b) TPA-2PQx devices; diode III (- - -) and diode IV (–).

TPA-2PQx means that the electrically generated ICT excited state responsible for EL is formed by recombination of the radical cation on the triphenylamine moiety with the radical anion on the phenylquinoline or phenylquinoxaline moiety.

Typical luminance−current density−voltage characteristics of OLEDs made from TPA-2PQ and TPA-2PQx are exemplified in Figure 6. The electroluminescence properties, including turn-on voltage, EL emission maximum, luminance, maximum current density, luminous efficiency (cd/A), and external quantum efficiency (EQE, %) are summarized in Table 2. The performance of the single-layer devices (diode I) was poor for both TPA-2PQ- and TPA-2PQx-based diodes, obtaining brightnesses of 15−30 cd/m^2 and EQE of less than 0.008%. This indicates inadequate charge-carrier utilization in the single-layer diodes, with most of the holes and electrons passing through the device with no recombination. As expected, the performance of these oligomers as emitters in OLEDs was greatly improved by using additional layers to facilitate the injection, transport, and confinement of electrons and holes (Table 2). An energy-level diagram showing all the HOMO and LUMO levels relevant to our OLEDs is shown in Figure 7. Devices using poly(*N*-vinylcarbazole) (PVK) (diode II) or 1,1-bis(4-tolylaminophenyl)cyclohexane (TAPC) (diode IV) as a hole-transport/electron-blocking layer (HTL) showed a turn-on voltage of 2.7−4.0 V, at which uniform emission over the whole pixel was visible to the eye. For each oligomer emitter, the performance of diode IV was superior to that of diode II, implying that TAPC (IP = 5.4 eV)[10a] is better at facilitating hole injection/transport while confining electrons to the emitter than PVK (IP = 5.8 eV).[10a] For TPA-2PQ diodes, device IV (TAPC) combined a lower turn-on voltage (2.7 V) with a higher maximum luminance of 3690 cd/m^2 (at 7.3 V) and a maximum 1.4% EQE (at 2510 cd/m^2 and 2.2 cd/A). In the case of TPA-2PQx diodes, device IV with a 2.5 V turn-on voltage, a maximum brightness of 4010 cd/m^2 (at 7.7 V) and a 1.2% EQE (at 1330 cd/m^2) is clearly superior to device II. The electroluminescence spectra were stable and similar to those of the single-layer diodes over a range of applied potentials (4−8 V), with a λ_{max}^{EL} of 464 nm and CIE (0.19, 0.23) for TPA-2PQ and a λ_{max}^{EL} of 506 nm and CIE (0.18, 0.48) for TPA-2PQx.

The overall performance of OLEDs employing these oligomers as emitters was substantially enhanced by the introduction of 1,3,5-tris(*N*-phenylbenzimidizol-2-yl)benzene (TPBI, IP = 6.2−6.7 eV)[3d] as a hole-blocking layer to confine holes to the ambipolar oligomer emitters. The EL results for diodes III and V are exemplified in Figure 6 and summarized in Table 2. The EL spectra of the TPA-2PQ- and TPA-2PQx-based diodes III and V were spectrally identical to those of the corresponding single-layer devices (diode I) and the respective thin-film PL emission spectra. Oligoquinoline-based OLEDs gave the best performance in device V, showing a maximum brightness of 6850 cd/m^2 (at 8.1 V) and a maximum luminous efficiency of 2.7 cd/A at 1390 cd/m^2 and 1.5% EQE. OLEDs based on the oligoquinoxaline emitter achieved their best performance in device III in terms of EL efficiencies, with a luminous efficiency of 7.9 cd/A at 310 cd/m^2 and a 3% EQE. The same diode III architecture had a maximum brightness of 8520 cd/m^2. However, TPA-2PQx diodes attained their brightest emission in diode V, which gave luminances of up to 15330 cd/m^2 and a maximum luminous efficiency of 5.5 cd/A (at 1090 cd/m^2 and 2.1% EQE).

A striking feature of these OLED performance results is that TPA-2PQx is observed to be a brighter and more efficient emitter than TPA-2PQ, despite its lower fluorescence quantum yield. The superiority of TPA-2PQx as an emitter was seen in all OLEDs tested, ranging from the

Table 2. Device Characteristics of OLEDs[a] Based on Oligomers TPA-2PQ and TPA-2PQx

oligomer	device[b]	V_{on}[c]	drive voltage (V)	current density (mA/cm^2)	luminance (cd/m^2)	device efficiency (cd/A), %EQE,[d]	λ_{max}^{EL} (nm)
TPA-2PQ (**3**)	I	2.7	6.9	366	14	0.004, 0.003	466
	II	4.0	10.4	322	1990	0.61, 0.29	467
			9.1	*75*	*680*	*0.93, 0.44*	
	III	4.1	10.7	291	3540	1.2, 0.69	469
			9.3	*75*	*1345*	*1.8, 0.98*	
	IV	2.7	7.3	219	3690	1.7, 1.0	464
			6.6	*112*	*2510*	*2.2, 1.4*	
	V	2.3	8.1	400	6850	1.7, 0.95	465
			6.1	*52*	*1390*	*2.7, 1.5*	
TPA-2PQx (**6**)	I	3.2	11.1	378	29	0.008, 0.007	505
	II	3.5	9.9	241	3000	1.3, 0.50	506
			6.7	*6.2*	*160*	*2.8, 1.08*	
	III	4.2	11.8	233	8520	3.7, 1.4	508
			8.0	*3.9*	*310*	*7.9, 3.0*	
	IV	2.5	7.7	256	4010	1.6, 0.63	506
			5.9	*42*	*1330*	*3.1, 1.2*	
	V	2.5	9.2	500	15330	3.0, 1.1	506
			6.4	*20*	*1090*	*5.5, 2.1*	

[a] Values in italic correspond to those for maximum device efficiencies at a practical brightness of at least >100 cd/m^2. [b] Device I: ITO/oligomer/LiF/Al; device II: ITO/PEDOT/PVK/oligomer/LiF/Al; device III: ITO/PEDOT/PVK/oligomer/TPBI/LiF/Al; device IV: ITO/PEDOT/TAPC/oligomer/LiF/Al; device V: ITO/PEDOT/TAPC/oligomer/TPBI/LiF/Al. [c] Turn-on voltage (at which EL is visible to the eye). [d] EQE = External quantum efficiency.

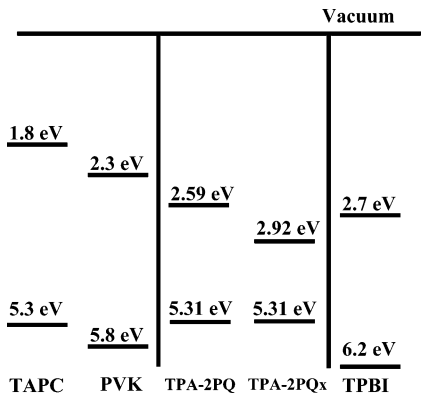

Figure 7. Energy levels (EA/IP) of the emissive oligomers (TPA-2PQ and TPA-2PQx) and hole or electron-blocking materials (TAPC, PVK, TPBI) used in the OLEDs.

single-layer devices where TPA-2PQx has a 2-fold advantage in brightness and device efficiency to diodes III, where TPA-PQx devices had a factor of 2−3 better brightness and efficiency. The substantially larger device brightness and EL efficiency of the oligoquinoxaline compared to the oligoquinoline can be understood in terms of the 0.33 eV larger electron affinity of the former. As shown in the energy-level diagram in Figure 7, TPA-2PQx diodes are expected to exhibit a more balanced injection and flux of electrons and holes than in those based on the oligoquinoline emitter.

Conclusions

We have synthesized two n-type oligomers, oligoquinoline and oligoquinoxaline with triphenylamine donor endgroups, and investigated their electrochemical, photophysical, and electroluminescence properties. The oligomers TPA-2PQ and TPA-2PQx had efficient intramolecular charge-transfer fluorescence with quantum yields of 62 and 34%, respectively. Both oligomers displayed reversible electrochemical reduction and oxidation, demonstrating ambipolar redox properties. Bright (up to 15300 cd/m^2) and efficient (7.9 cd/A and 3.0% EQE) green OLEDs were realized from the oligoquinoxaline (TPA-2PQx) emitter. In contrast, electroluminescence from the oligoquinoline TPA-2PQ was blue-green in color with a maximum brightness of 6850 cd/m^2 and a luminous efficiency of 2.7 cd/A and a 1.5% EQE. The finding that the oligoquinoxaline is a far superior emitter in OLEDs than the oligoquinoline was explained by the 0.33 eV lower-lying LUMO, which facilitated a more efficient electron injection/transport and charge recombination. These results demonstrate that n-type oligomers with p-type endgroups represent a promising architecture for developing next generation ambipolar emitters for optoelectronics. Furthermore, the present oligomers are expected to be useful model systems for the related polyquinolines and polyquinoxalines.

Experimental Section

Materials. 3,3′-Dibenzoylbenzidine was synthesized according to literature methods.[22] Phenylacetylene, 4-bromo-*N*,*N*-diphenylaniline, palladium(II) acetate, CuI, triphenylphosphine, triethylamine, potassium permanganate, 3,3′-diaminobenzidine, and other chemicals were obtained from Aldrich and used as received.

Synthetic Procedures. *1-(4-Diphenylamino-phenyl)-ethanone (1).* Diphenylamine (6.18 g, 36.5 mmol), 4-bromoacetophenone (7.23 g, 36.3 mmol), bis(dibenzylidineacetone)-palladium(0) (0.44 g, 0.76 mmol), tri-*tert*-butylphosphine (0.30 g, 1.5 mmol), and potassium *tert*-butoxide (4.83 g, 43.0 mmol) were stirred overnight at 80 °C under static argon. The product was extracted into CH_2Cl_2, purified by silica gel chromatography using CH_2Cl_2/hexanes as an eluent, and recrystallized twice from CH_2Cl_2/hexanes. Yield was 75% as yellow crystals. T_m = 135 °C. ^{1}H NMR ($CDCl_3$): δ 7.81 (m, 2H), 6.81 (m, 12H), 2.12 (s, 3H). FT-IR (KBr, cm^{-1}): 3332, 3037, 1754, 1672, 1584, 1506, 1489, 1451, 1424, 1359, 1335, 1319, 1272, 1189, 1179, 1123, 1075, 1028, 958, 901, 838, 757, 729, 698, 678, 639, 623. HRMS (FAB) calcd for $C_{20}H_{17}NO$, 287.36; found, 287.36.

2,2′-Bis(triphenylamine)-4,4′-diphenyl-[6,6′]biquinoline (3). 1-(4-diphenylamino-phenyl)-ethanone (**1**; 2.2 equiv), 3,3′-dibenzoylbenzidine (1 equiv), diphenyl phosphate (3 g), and toluene (2 mL) were

(22) (a) Agrawal, A. K.; Jenekhe, S. A. *Macromolecules* **1993**, *26*, 895. (b) Tonzola, C. J.; Alam, M. M.; Bean, B. A.; Jenekhe, S. A. *Macromolecules* **2004**, *37*, 3554.

stirred under static argon at 140 °C for 24 h. The reaction mixture was precipitated into 10% triethylamine/methanol. The precipitate was collected by vacuum filtration, filtered through silica gel to remove polar byproducts, and then recrystallized twice from a CH_2Cl_2/hexanes mixture of approximately 40−50% hexanes. Yield was 68% as a dark red solid. T_m = 330 °C. ^{1}H NMR ($CDCl_3$): δ 8.15 (m, 6H), 7.91 (s, 2H), 7.60 (t, 10H), 7.36 (m, 8H), 7.20 (m, 20H). FT-IR (KBr, cm^{-1}): 3448, 3057, 3032, 2922, 2850, 1586, 1560, 1555, 1542, 1541, 1521, 1483, 1457, 1448, 1437, 1428, 1331, 1286, 1777, 820, 758, 716, 697, 621. HRMS (FAB) calcd for $C_{66}H_{46}N_4$, 895.13; found, 895.30.

Diphenyl-(4-phenylethynyl-phenyl)-amine (4). 4-Bromo-*N*,*N*-diphenylaniline (8.0 g, 25.0 mmol), palladium(II) acetate (56 mg, 0.25 mmol), CuI (95 mg, 0.5 mmol), triphenylphosphine (131 mg, 0.5 mmol), and triethylamine (150 mL) were mixed together under an argon atmosphere. Phenylacetylene (3.3 g, 32.5 mmol) was then added. The mixture was stirred at 80 °C under argon for 10 h. After removal of triethylamine under reduced pressure, the residue was dissolved in dichloromethane, washed with brine, dried over sodium sulfate, and concentrated. The crude product was purified by silica gel column chromatography using 2% ethyl acetate in hexane as eluent. Viscous oil (6.9 g) was obtained with 81% yield. ^{1}H NMR (300 MHz, $CDCl_3$): δ 7.54−7.58 (m, 2H), 7.29−7.45 (m, 9H), 7.05−7.18 (m, 8H). GC-MS showed the presence of only one component with *m*/*z* 345.

1-(4-Diphenylamino-phenyl)-2-phenyl-ethane-1,2-dione (5). Compound **4** (7.0 g, 20.0 mmol) was dissolved in dichloromethane (100 mL). To this solution was added Adogen464 (0.4 g), potassium permanganate (12.6 g, 80.0 mmol), sodium bicarbonate (1.6 g), and water (100 mL). The mixture was stirred vigorously at room temperature overnight. The reaction was quenched with sodium hydrogen sulfite and HCl. The solution was extracted with methylene chloride. The combined organic layers were dried over anhydrous sodium sulfate, and the solvent was removed by rotary evaporation. The crude product was purified by column chromatography using 10% ethyl acetate in hexane as eluent. Viscous oil (4.8 g) was obtained with 63% yield. ^{1}H NMR (300 MHz, $CDCl_3$): δ 7.99 (d, 2H), 7.81 (d, 2H), 7.66 (t, 1H), 7.52 (t, 2H), 7.21−7.36 (m, 10H), 6.97 (d, 2H). GC-MS showed the presence of only one component with *m*/*z* 377.

2,2′-Bis(triphenylamine)-3,3′-diphenyl-[6,6′]biquinoxaline (6). A mixture of compound **5** (300 mg, 0.8 mmol), 3,3′-diaminobenzidine (68 mg, 0.32 mmol), potassium carbonate (88 mg, 0.64 mmol), and ethanol (40 mL) was refluxed under an argon atmosphere for 10 h. After removal of ethanol under reduced pressure, the residue was dissolved in dichloromethane, washed with brine, dried over sodium sulfate, and concentrated. The crude product was purified by silica gel column chromatography using 25% ethyl acetate in hexane as eluent. Recrystallization from ethyl acetate gave 161 mg (45%) of **6** as bright yellow solid. ^{1}H NMR (300 MHz, $CDCl_3$): δ 8.63 (s, 2H), 8.32 (d, 2H), 8.22 (d, 2H), 7.65 (m, 4H), 7.02−7.44 (m, 34H). FT-IR (KBr pellet, cm^{-1}): 3058, 1591, 1510, 1492, 1342, 1280, 1178, 1058, 1028, 841, 754, 696. FAB MS: *m*/*z* 897 (M^+).

Characterization. FT-IR spectra were taken on a Perkin−Elmer 1720 FTIR spectrophotometer with KBr pellets. ^{1}H NMR spectra were recorded on a Bruker-AV301 spectrometer at 300 MHz. GC-MS spectra were obtained on a Hewlett−Packard 5971 GC/mass spectrometer or Bruker Esquire LC/ion trap mass spectrometer. Differential scanning calorimetry (DSC) analysis was performed on a TA instrument Q100 under N_2 at a heating rate of 10 °C/min. Thermogravimetric analysis (TGA) analysis was conducted with a TA instrument Q50 at a heating rate of 20 °C/min under a nitrogen gas flow.

Cyclic Voltammetry. Cyclic voltammetry experiments were done on an EG&G Princeton Applied Research potentiostat/galvanostat (model 273A). Data were collected and analyzed by the Model 270 electrochemical analysis system software on a PC computer. A three-electrode cell was used in all experiments. Platinum wire electrodes were used as both counter and working electrodes and silver/silver ion (Ag in 0.1 M $AgNO_3$ solution, Bioanalytical System, Inc.) was used as a reference electrode. The Ag/Ag^+ ($AgNO_3$) reference electrode was calibrated at the beginning of the experiments by running cyclic voltammetry on ferrocene as the internal standard in an identical cell without any oligomer on the working electrode. The potential values obtained in reference to the Ag/Ag^+ electrode were converted to the saturated calomel electrode (SCE) scale. Solution electrochemistry was performed on 2 mM solutions of each oligomer in 1.5:1 (v/v) benzene: acetonitrile mixture solvent. An electrolyte solution of 0.1 M $TBAPF_6$ in acetonitrile was used in the electrochemical cell. The solutions were purged with ultrahigh purity N_2 for 10−15 min before the experiment, and a blanket of N_2 was used during the experiment. Electrochemistry was done at a scan rate of 200 mV/s.

Time-Resolved Photoluminescence Decay Dynamics. Fluorescence decays of the compounds in solution and as thin films were obtained on a PTI Model QM-2001-4 spectrofluorimeter equipped with a Strobe Lifetime upgrade. The instrument utilizes a nanosecond flash lamp filled with a high-purity nitrogen/helium (30/70 v/v) mixture as the excitation source and a stroboscopic detection system. The decay curves were analyzed using a software package provided by the manufacturer. Reduced chi-square values, Durbin−Watson parameters, and weighted residuals were used as the goodness-of-fit criteria. All measurements were done in ambient conditions at room temperature.

Fabrication and Characterization of OLEDs. We fabricated OLEDs using TPA-2PQ and TPA-2PQx as the emissive materials. Indium−tin oxide (ITO)-coated glass substrates (Delta Technologies Ltd., Stillwater, MN) were cleaned sequentially in ultrasonic baths of a 2-propanol/deionized water (1:1 volume) mixture, toluene, deionized water, and acetone. The substrates were then dried at 60 °C in a vacuum overnight. An ∼1 wt % poly(ethylenedioxythiophene)/poly(styrene sulfonate) blend (PEDOT) dispersion in water was filtered through a 0.45 μm poly(vinylidene fluoride) (PVDF) syringe filter. A 50 nm thick layer was then spin-cast onto the ITO-coated glass to act as a hole-injection layer and dried at 200 °C for 15 min under vacuum. A 20 nm thick hole-transport/electron-blocking (HTL) (PVK or TAPC) was later spin-coated from its 1 wt % toluene solution onto the PEDOT layer and dried at 60 °C for 4 h under vacuum. Forty to fifty nanometer thick films of each oligomer were evaporated from resistively heated quartz crucibles at a rate of 0.2−0.4 nm/s in a vacuum evaporator (Edwards Auto 306) at a base pressure of $<3 \times 10^{-6}$ Torr onto the HTL. Subsequently, a 25 nm thick hole blocking layer (TPBI) was evaporated onto the oligomer layer. The chamber was vented with air to load the cathode materials and pumped down to $\sim 2 \times 10^{-6}$ Torr; a 2 nm thick lithium fluoride layer followed by an 120 nm thick aluminum layer were deposited through a shadow mask to form active diode areas of 0.2 cm^2. The film thicknesses were measured by an Alpha-Step 500 surface profiler (KLA Tencor, Mountain View, CA). Electroluminescence spectra were obtained using a PTI QM-2001-4 spectrophotometer. Current−voltage characteristics of the OLEDs were measured using a HP4155A semiconductor parameter analyzer (Yokogawa Hewlett−Packard,

(23) (a) Kulkarni, A. P.; Jenekhe, S. A. *Macromolecules* **2003**, *36*, 5285. (b) Okamoto, S.; Tanaka, K.; Izumi, Y.; Adachi, H.; Yamaji, T.; Suzuki, T. *Jpn. J. Appl. Phys.* **2001**, *40*, L783.

Tokyo). The luminance was simultaneously measured using a model 370 optometer (UDT instruments, Baltamore, MD) equipped with a calibrated luminance sensor head (model 211) and a 5× objective lens. The device external quantum efficiencies were calculated using procedures reported previously.[23] All the device fabrication and characterization steps were done under ambient laboratory conditions.

Acknowledgment. This research was supported by the NSF (CTS-0437912), the NSF STC MDITR (DMR-0120967), and an NSF IGERT Nanotechnology Fellowship Award to J.M.H. from the Center of Nanotechnology at the University of Washington.

CM0613760